HHS Public Access

Author manuscript

J Neural Eng. Author manuscript; available in PMC 2018 December 01.

Published in final edited form as:

J Neural Eng. 2017 December ; 14(6): 066005. doi:10.1088/1741-2552/aa7a42.

A novel flexible cuff-like microelectrode for dual purpose, acute and chronic electrical interfacing with the mouse cervical vagus nerve

A S Caravaca[1,*], **T Tsaava**[2,*], **L. Goldman**[3,*], **H. Silverman**[2], **G. Riggott**[4], **S S Chavan**[2], **C Bouton**[3], **K J Tracey**[3,4], **R Desimone**[4,#], **E S Boyden**[5,#], **H S Sohal**[3,#], and **P S Olofsson**[1,#]

[1]Karolinska Institutet, Department of Medicine, Solna, Center for Molecular Medicine, Center for Bioelectronic Medicine, Karolinska University Hospital, Stockholm, Solna, Sweden

[2]Feinstein Institute for Medical Research, Laboratory of Biomedical Science, Manhasset, New York, USA

[3]Feinstein Institute for Medical Research, Center for Bioelectronic Medicine, Manhasset, New York, USA

[4]Massachusetts Institute for Technology, Cambridge, Massachusetts, USA

[5]Massachusetts Institute for Technology, Media Lab, Cambridge, Massachusetts, USA

Abstract

Objective.—Neural reflexes regulate immune response and homeostasis. Advances in bioelectronic medicine indicate that electrical stimulation of the vagus nerve can be used to treat inflammatory disease, yet the understanding of neural signals that regulate inflammation is incomplete. Current interfaces with the vagus nerve do not permit effective chronic stimulation or recording in mouse models, which is vital to studying the molecular and neurophysiological mechanisms that control inflammation homeostasis in health and disease. Here, we developed an implantable, dual purpose multi-channel, flexible electrode array, a “microelectrode”, for recording and stimulation of the mouse vagus nerve.

Approach.—The array was microfabricated on an 8 μm layer of highly biocompatible parylene configured with 16 sites. The microelectrode was evaluated by studying the recording and stimulation performance. Mice were chronically implanted with devices for up to 12 weeks.

Main Results.—Using the microelectrode in vivo, high fidelity signals were recorded during physiological challenges (e.g potassium chloride and interleukin-1 β), and electrical stimulation of the vagus nerve produced the expected significant reduction of blood levels of tumor necrosis factor (TNF) in endotoxemia. Inflammatory cell infiltration at the microelectrode implantation at 12 weeks of implantation was limited in our radial distribution analysis of inflammatory cell.

Significance.—This novel device provides an important step towards a viable chronic interface for cervical vagus nerve stimulation and recording in mice for both acute and chronic applications.

peder.olofsson@ki.se, hsohal@northwell.edu.

*= First co-authors

#= Final Contributing authors

Introduction

Bioelectronic medicine, an emerging interdisciplinary field, brings molecular biology and neurotechnology together to use electrical devices as therapeutic agents to treat disease by targeting specific molecular mechanisms through delivery of electrical impulses to defined neural circuits [1–3]. There is increasing evidence that neural reflex circuits modulate innate and adaptive immunity [4]. The “inflammatory reflex” is a well- defined neural circuit in which action potentials transmitted in the vagus nerve play a key role to regulate inflammation [5,6]. This pathway can be activated by electrical stimulation of the cervical vagus nerve. Vagus nerve stimulation significantly attenuates pro-inflammatory cytokine levels in experimental disease, and murine disease models have been used to map the neurophysiology of the efferent arc of the inflammatory reflex in detail [7,8]. The resulting discoveries have spawned human clinical trials using implanted devices for electrical stimulation of the vagus nerve for treatment of chronic diseases such as rheumatoid arthritis and Crohn’s disease with encouraging results [9,10].

However, the optimal parameters for vagus nerve stimulation in inflammatory diseases have not been established, in part because technology for chronic implantation of electrodes in relevant mouse models has been lacking. For the same reason, the neurophysiology of long-term electrical vagus nerve stimulation has not been mechanistically addressed. It is likely that electrodes suitable for chronic implantation in mice would significantly improve our ability to optimise stimulation parameters in chronic inflammatory diseases.

In addition, little is known about the electrical activity in the sensory, afferent arc of the inflammatory reflex. The vagus nerve relays signals on cytokine levels in the periphery to the central nervous system [11,12], but studying the neurophysiology of these afferent signals has been challenging. Recent discoveries suggest that the vagus nerve transmits action potentials of specific neural signatures in response to specific cytokines [13]. Chronic electrode implants capable of recording detailed electrical activity of the vagus nerve would enable testing the hypothesis that defined inflammatory conditions elicit identifiable electrical signatures in the vagus nerve [1,13].

Mice have long served as experimental models in understanding human pathologies and together with development of transgenic mice, have propelled research and investigation of molecular mechanisms underlying the onset of disease to discovery of prevention and treatment of disease (Vandamme 2014). Mice have been made the choice for genetic experimentation over many decades as they are inexpensive to maintain compared to other rodents whilst being prolific breeders, making “humanized “ genetically engineered mice prone to a wide range of immunodeficiencies valuable for biomedical exploration and discovery (Rosenthal and Brown 2007). A chronic electrode would further expand our knowledge of disease pathogenesis over time, while allowing for potential treatment optimization by monitoring homeostatic imbalance and regulation.

To understand and to perturb signals in the mouse cervical vagus nerve has been challenging in both acute and chronic interfacing. Many current electrode designs have low channel counts allowing the capture of only a certain number of compound action potentials (CAPs)

to any given pharmacological challenge of the nerve. Further, many of these implants can not be successfully implanted chronically due to their size and can damage the nerve long-term [9]. Chronic implants allow for repeated measurements of activity from the nerve in healthy and disease models to formulate a signature electrical footprint for certain disease states, an important step in bioelectronic medicine and neuromodulation.

The implicit design challenges of interfacing with the mouse cervical vagus nerve include - successfully wrapping around a cuff that causes minimal damage to the nerve and ensuring good electrical contact, which is of around 100 μm in diameter. Further, routing the connections from the electrodes to an appropriate connector, without placing unnecessary tethering forces on the nerve to damage it over time is another tremendous challenge.

A microfabrication process was already developed for flexible, highly biocompatible probes intended for intracortical use and capable of stably recording electrical activity in the rabbit cortex for a period exceeding two years [16–18]. To our knowledge, this technology has not yet been implemented for interfacing with peripheral nerves. Here, we set out to use the thin film parylene-C microfabrication technology for development of a multichannel microelectrode suitable for chronic implantation, electrical stimulation, and recording of electrical activity in the mouse vagus nerve.

Materials and Methods

The 16 electrode sites were configured on a 2 mm × 3 mm, 8 urn thick parylene sheet in different arrangements. The electrodes were spaced in a 350 μm wide region to accommodate for the circumference of the mouse cervical vagus nerve, which commonly is ~350–380 μm. Electrode site areas were 6400, 2500 or 225 μm^2. The arrangement of electrode sites were either tetrode-like (Figure 1A) or diagonal (Figure 1B). The oversize flap design facilitates ease-of-handling during surgery and secure placement of the device in the mouse. In some designs, two macro-stimulation sites were placed at either end of the microelectrode with recording sites located in between. To mechanically decouple the microelectrode from the larger interfacing ribbon cable (3 cm long, 3 mm wide), the design had a ‘necking region’ to accommodate the movement of the nerve relative to the microelectrode to attenuate long-term insult to the nerve. The ribbon cable contained bond pads that allowed interfacing to commercial Omnetic nanoseries connectors (NPD-18-AA-GS, Omnetics Corporation, USA) used to interface with electrophysiological set-ups (Figure 1C).

Electrode Microfabrication and Wiring

Electrode microfabrication followed previously optimised process flows used for parylene-C and tungsten-titanium (WTi) technology [16,17]. In short, the microelectrode consisted of a parylene-C (4 μm)-WTi (300 nm)-parylene-C (4 μm) sandwich. WTi was etched with SF_6 reactive ion etch (RIE) to define the metal traces, electrode sites and bondpad regions. The parylene-C insulating layers were simultaneously etched using O_2 RIE to define the overall body of the electrode and to re-open the recording sites and bondpad regions.

For device release from the carrier wafer previous process flows used aluminum etched by TMAFI. However, in this generation, HF (1:10 49% HF) released devices a lot faster (typically under one minute), to minimise the exposure of the parylene-C based devices to wet etchants, which could cause abnormalities in the layers (e.g. polymer swelling) [17].

Connectors were bonded to the corresponding WTi bondpads under a stereoscope. Silver epoxy was applied to the connector, aligned and placed on the metal bondpads [17]. Successful electrical connections were confirmed through impedance measurements at 1 kHz in physiological saline using an IMP 2C impedance meter (Microprobes, USA). The connector was insulated using two-part epoxy.

Ethics Statement

This study and all experimental protocols therein were approved by the Institutional Animal Care and Use Committee (IACUC) at the Feinstein Institute for Medical Research, Northwell Health System (Manhasset, NY, USA), which follows the National Institute of Health (NIH) guidelines for the ethical treatment of animals and the Stockholm Regional Board for Animal Ethics (Stockholm, Sweden).

Animals

We used male BALB/c (age 8–12 weeks) and C57Bl/6J (8–12 weeks) mice purchased from Charles River Laboratories. They were housed in a laboratory environment on a 12-h light and dark cycle at 25°C, with *ad libitum* access to food and water.

Microelectrode Implantation

Following the induction of isoflurane, the mouse was placed in the supine position and a ventral midline cervical incision was performed between the mandible and sternum. Subcutaneous tissues were retracted laterally to expose the mandibular salivary glands. A gauze pad was placed over the incision and the mouse was placed in the prone position. A dorsal midline incision was made and subcutaneous tissues were retracted laterally. The integrated cable was subcutaneously tunneled from the back of the mouse back towards the midline cervical incision. The mouse was placed back into the supine position and the salivary glands were bluntly separated and retracted away from the operative field. Proper exposure revealed the left neurovascular bundle containing the cervical vagus nerve, which was dissected away from the vasculature and isolated between the sternomastoid and sternohyoid muscles before being immobilized with a suture. The microelectrode was placed under the nerve, folded over and sutured to secure its place. The connector was fixed to head of the Mouse. Mice were recovered on a heating pad until they gained adequate righting reflex and returned to the home cage.

Vagus Nerve Stimulation

Electrical stimulation of the left cervical vagus nerve was performed using a stimulation module (Plexon, TX, USA) set at current control, 1 mA, 250 μs biphasic pulse, 50 μs interphase delay, 10 Hz, for 60 seconds. Mice in the sham group were subjected to surgery, but no electrical stimulation. After 3 h of recovery, 5 mg/kg endotoxin was administered intraperitoneally (endotoxin from *Escherichia coli,* 0111 :B4; Sigma- Aldrich, MO, USA).

Mice were euthanized 90 minutes post-injection and serum was analysed for levels of tumor necrosis factor alpha (TNFα) by ELISA (R&D Systems) performed according to manufacturer instructions.

In Vivo Recording

In spontaneously breathing mice under isoflurane anesthesia, electrical activity was sampled at 30 kHz using a RHD 2000 evaluation system (Intan Technologies, USA) using a unipolar recording set-up, with the reference wire placed in the contralateral salivary gland. A software 200 Hz high-pass filter was applied to the active channels, and the 'spike-scope' feature used in the bundled software for real-time visualisation of CAPs. Baseline activity was acquired for 30 minutes. Under isoflurane the heart rate was approximately 368 beats per minute ± 19.8 and respiratory rate was approximately 54.3 breaths per minute ± 7.0. During continuous acquisition, mice were subjected to (1) 50 uL of potassium chloride (KCI; 4 mM) application directly applied on top of the vagus nerve with a parafilm trough underneath the nerve to prevent spreading to other structures (2) intraperitoneal injection of 200 uL of physiological saline or (3) intraperitoneal injection of 200 uL of interleukin-1 β (IL-1 β; 350 ng/mg; eBioscience, CA) in physiological saline.

Recorded raw data was imported into Offline Sorter (Plexon, USA), where a 200 Hz high pass filter was applied to extract the frequency band of interest for CAPs. Principal Component Analysis (PCA) was utilised for CAP sorting. A threshold crossing was set to capture most of the potential CAPs and include some 'noise' to supply a defined noise profile in the PCA space to contrast with identified features. The threshold level was set by taking the median of the mean bandpassed signal/0.6745 (σ). The threshold was set at 4σ (Quiroqa et al. 2004). Saved features, including waveforms and 'spike' timings, were imported into Matlab (2014b, Mathworks, USA), for further analysis. Mean peak-to-peak signal, noise and signal-to-noise ratio (SNR) were measured using custom-written scripts. Further metrics, such as CAPs per channel were also calculated and CAPs corresponding to the subsequent 'bursting' of activity from vagus nerve activity after IL-1 β injection were isolated from the 200 Hz high passed signal.

Immunohistochemistry

Immunohistochemistry was used to assess tissue response to implanted microelectrodes. Under CO_2 anesthesia, mice were perfused transcardially with phosphate buffered saline (PBS) and paraformaldehyde 4% in PBS. Samples were embedded in an optimal cutting temperature (OCT) compound and frozen over dry ice. 10-μm sections were cut on a cryostat, mounted on slides (Superfrost, Thermo Fisher Scientific) and dried.

Slides were incubated for 30 minutes at room temperature in blocking buffer (5% normal horse serum, Tris-buffered saline (TBS), 0.1% Tween 20) and then 3% hydrogen peroxide solution for 15 minutes. Samples were stained with anti-CD3 antibody (500 A2, eBioscience, 1:75) and anti-l-Ab antibody (KH74, BD Pharmingen, 1:300). Primary antibodies were diluted in antibody diluent (5% normal horse serum, TBS, 0.1% Tween 20) overnight at 4°C. The following day after washing in wash buffer (TBS 0.1% Tween 20) anti-CD3 was incubated with in anti-hamster biotinylated secondary antibody (1:200)

diluted in antibody buffer and anti-l-Ab was incubated in antibody buffer for 30 minutes at room temperature. Diaminobenzidine (DAB, Vector Laboratories) followed by counterstaining with haematoxylin staining was used. Images were captured with a Leica Microsystems DMRB microscope.

Images were analysed in the Matlab environment (2014b Mathworks, USA) as previously described [18]. In brief, image intensities were normalized to the endogenous background staining for each slide. Radial distribution intensity measurements, centered on the nerve were measured concentrically, every 2 μm, with measurements obtained up to 150 μm from the identified nerve center.

Statistics

Data are expressed as mean +/− SEM. Differences in cytokine levels between groups were analysed using unpaired two-tailed Student's *t*-test (Prism 7.0, GraphPad software, San Diego, CA, USA). Differences in radial distribution intensities were analysed using paired, two-tailed Student's *t* test. $p<0.05$ was considered significant.

Results

Electrode Impedance

Electrode impedance as measured at 1 kHz in physiological saline was 100±12, 411 ±21, and 910±75 kΩ for 6400, 2500 and 225 μm^2 recording sites, respectively (n=320 sites). The impedance values indicate that the microfabrication process between the different electrode designs was stable and consistent.

Vagus nerve recordings using microelectrodes capture high fidelity compound action potentials

A microelectrode was implanted around the left cervical vagus nerve in an anesthetized mouse and baseline activity recorded for 30 minutes (Figure 2A). To investigate the maximal number of features obtainable by the recording electrodes, 50 μL of 4 mM KCI was applied directly on top of the vagus nerve to fully depolarise it (Figure 2B). Parafilm was placed underneath the nerve before application to prevent the spread of KCI to surrounding structures. Data was acquired continuously for an additional 30 minutes after KCI application. We observed an increase in overall electrical activity and obtained a good number of CAPs across all recording channels (Figure 2C, Mean±SEM CAPs = 2.36±0.50 per channel). Further, clear separation of CAPs were observed in the PCA space (data not shown). High fidelity signal (477±38 μV) and SNR (8.63±1.36) was obtained from the 2500 μm^2 sites (Figure 2D). Good signal quality (179.5±24.5 μV) and SNR (5.98±0.81) with 3.25±0.45 features per channel were obtained from the 6400^2 μm sites (Figure 2E). The impedance of the 225 μm^2 sites was too high to allow for meaningful CAP isolation over the noise band (data not shown).

No change in vagus nerve activity observed upon saline challenge

In anesthetized mice implanted with a microelectrode on the left vagus nerve, 200 μL of saline was injected intraperitoneally during continuous electrophysiological acquisition. At

the point of injection (time '0' seconds), an acute increase of activity lasting less than 3 seconds was observed. No change in amplitude and frequency of the recorded signal was observed after saline injection as compared to baseline which was consistent across all animals. The electrical activity associated with the cardiac and respiratory cycles also remain unchanged (Figure 3).

Vagus nerve compound action potentials associated with injection of IL-1 β Intraperitoneal injection of IL-1 β in mice has been described to elicit an electrical response measurable by electrodes on the cervical vagus nerve [13]. Pharmacological challenges can evoke compound action potentials (CAPS) as previously described for example by Niijima (A. Niijima 1982; Akira Niijima 1994). The waveforms recorded from the surface electrodes in this study show distinct waveforms (triphasic, monophasic, biphasic) and time course (~3 ms) consistent with compound action potentials. To evaluate whether these microelectrodes are capable of capturing the CAPs elicited by IL-1 β injection, a subset of mice were injected intraperitoneally with 200 μL (350 ng/mg) IL-1 β after a 30 minute baseline recording (Figure 4A). Compared with baseline, distinctive CAP shapes and interspike intervals were observed in the bursts 5 minutes after injection (Figure 4B-D). These bursts were only found in a subset of the 14 adjacently arranged recording channels spaced 250 μm apart.

Recorded 'spike' times were used to calculate the delay between the specific features being picked up on the channels. This information enables calculation of the conduction velocity of the given features and deduction of the likely type of fibres involved in the response (Figure 4C). For example, the difference between a burst-associated feature captured across two sites spaced 250 μm apart, was 6 ms. This corresponds to a conduction velocity of 42 m/s. Another feature captured across two channels had a 12 ms difference in times, which equates to a 21 m/s conduction velocity (Figure 4D). The longitudinal configuration of the microelectrode also permits using spike times for specific features to determine directionality, i.e. whether a feature represents an efferent or afferent signal propagation. Thus, capturing burst-associated CAPs on multiple channels can be a tool to determine which specific fiber types are likely involved in a response.

Electrical stimulation of the cervical vagus nerve using the microelectrode reduced TNFα in endotoxemia

Vagus nerve stimulation of the cervical vagus nerve is known to trigger activation of the inflammatory reflex, suppressing endotoxin-induced TNFα levels [7,19,20]. To investigate whether this microelectrode design permits activation of the inflammatory reflex, we studied vagus nerve stimulation in an established model of endotoxemia. Mice were anesthetized and implanted with a microelectrode on the left cervical vagus nerve. Electrical stimulation through the microelectrode was applied for 60 s using the following settings: 1 mA output current, 250 μs biphasic pulse width duration, 50 μs interphase delay, at a 10 Hz pulse frequency. Three hours after this stimulation, 5 mg/kg endotoxin was injected intraperitoneally. Mice were euthanized 90 minutes later and serum collected and analysed for TNFα. The TNFα levels were significantly lower in the electrically stimulated mice as

compared to sham-operated controls (n=30; $p<0.05$), validating the design capability to activate the cholinergic anti-inflammatory pathway [19] (Figure 5).

Minimal foreign body response elicited by the implanted microelectrode

Anesthetized mice were implanted with a microelectrode on the left cervical vagus nerve. The left cervical vagus nerve along with surrounding tissues were harvested 12 weeks after implantation. Presence of CD3 and l-Ab, molecules associated with inflammation, was determined by immunohistochemistry. No significant differences in either CD3 or l-Ab staining were found between non-implanted and implanted nerve areas (Figure 6) as determined by normalised radial distribution analysis extending 150 um from the cross-sectional nerve center [18]. The limited inflammatory response observed indicates high biocompatibility of the implanted microelectrode.

Discussion

Here, we present a novel, high density, customisable, 16 channel microelectrode intended for both acute and chronic stimulation and recording of the electrical activity in the mouse cervical vagus nerve. The microelectrode is based on thin film parylene-C technology, equipped with a ribbon cable, external connector and other features to facilitate secure positioning of the microelectrode in vivo.

The ultra-thin, inherently flexible, and customisable design of the microelectrode developed in this study allows for improved interfacing with small diameter peripheral nerves in mice and avoids the increased tissue pressure associated with bulky silicone cuffs. Although silicone based electrodes have been used successfully in rats [31], even in the clinical setting [32–35], the inherent minute size and manipulation of the nerve, make it difficult for such a strategy to be employed chronically. In addition, nerve electrodes implanted in previous studies have induced inflammation around the nerve causing device degradation and failure, limiting the functionality in small animals due to mechanical damage and nerve injury [14]. In contrast, our chronic microelectrode implantation showed a minimal foreign body response over a 12 week period.

The microelectrode in this study was evaluated for recording and stimulation performance in mice, showing good feature detection during specific challenges (e.g. KCI and IL-1 β) and effective stimulation compared to sham-operated controls as shown in the well-characterized model of endotoxemia [9,20]. The reduction in TNFα in response to electrical vagus nerve stimulation is consistent with prior studies, and validates the stimulation capability of the microelectrode [7,20]. Since electrical activation of the vagus nerve is known to modulate experimental inflammatory diseases including sepsis, ischemia-reperfusion injury, inflammatory bowel disease, rheumatoid arthritis, and other conditions in which inflammation plays a role in the pathogenesis, this new technology promises to enable the study of acute and chronic disease models in mice for extended periods of time [3,9].

The unipolar recording setup using the microelectrode for the vagus nerve obtained high fidelity signals in response to a KCI challenge. A unipolar recording setup was used in order to determine the signal propagation velocities from the mouse cervical vagus nerve, which

would be difficult in other recording setups that would require larger exposure of the nerve in an otherwise limited surgical field.

A contributing factor to the high fidelity recordings was likely the greater adhesion to the nerve, in comparison to other common electrode materials, of flexible parylene-C [21], thereby increasing the electrical coupling for the recording sites. Previous studies of peripheral implants used for rodents have reported peak-to-peak signal amplitudes ranging from 100–900 μV in response to electrical stimuli [22–27]. In this study, recorded peak-to-peak signal amplitudes ranged between 100 and 2500 μV in response to pharmacological stimuli, and differed with the size of recording sites.

The recording from multiple channels configured in close proximity along and around the nerve enabled the observation that some isolated features were detected on some but not all channels, i.e detectable only in specific locations on the nerve. Using bipolar electrodes, Steinberg et al. [13] recently demonstrated cytokine-specific neurograms in the sensory vagus nerve in mice. In light of this, it is tempting to speculate that the multichannel microelectrode technology presented here could be used to improve resolution for detection of specific signatures of inflammation. The current device design is fabricated with 16 channels, but it can easily be scaled up to ~1000 channels with the use of previously established process flows [29]. We find it plausible that a high density electrode array would significantly improve interface performance.

Capturing multiple features across different channels allowed observation of the delay between channels of specific features, information that subsequently was used to calculate conduction velocities and directionality for propagation. Different fibre types in the peripheral nervous system are associated with specific conduction velocities [30,31]. Hence, information on signal propagation velocities may identify specific fibre types involved in a response, and indicate whether the activity is efferent or afferent. The histological analysis indicates that this microelectrode may be suitable for chronic implantation with limited risk for nerve damage, a considerable challenge for chronic interfacing. This is perhaps attributable to the multiple design measures to prevent unnecessary tethering stresses on the nerve - ultra-thin film design, necking region to decouple the ribbon cable from the microelectrode, and an incorporated ribbon cable to allow for stabilisation of the connector on the skull of the mouse.

The ability to combine effective simulation, high fidelity recording and chronic implantation in a single device, as we have shown, is potentially very useful for multiple experimental models used in bioelectronic medicine. Chronic implantation allows for the repeated acquisition of electrical signatures potentially associated with specific disease activity and, combined with stimulation, theoretically enables design of closed-loop systems for automated correction of aberrant activity through electrical nerve stimulation. Studies are ongoing to further characterise the recording and stimulation performance of the microelectrode in chronic mouse model settings.

Conclusions

Here, we present a novel, flexible, biocompatible, high channel count, cuff-like microelectrode designed for acute and chronic stimulation and recording of the mouse cervical vagus nerve. This technology aims to improve our ability to mechanistically dissect the neurophysiology and molecular biology of the reflex control of inflammation and provide stepping stones for the advancement of bioelectronic medicine.

Acknowledgements

We would like to thank Emily Battinelli, Harold Silverman and Dr. Valentin Pavlov at the Feinstein Institute for Medical Research, Manhasset, New York, U.S.A. for valuable input. This work was supported in part by NIH Director's Pioneer Award 1DP1NS087724, NIH 1R24MH106075, NIH 1R01MH103910, NIH 1R01EY023173, Knut and Alice Wallenberg's Foundation 20140212, Heart Lung Foundation 20150767, and New York Stem Cell Foundation Robertson Award.

References

1. Tracey KJ. Shock Medicine. Sci Am. 2015 2 17;312(3):28–35.
2. Chow BY, Boyden ES. Optogenetics and translational medicine. Sci Transl Med. 2013 3 20;5(177): 177ps5.
3. Bonaz B, Sinniger V, Pellissier S. Anti-inflammatory properties of the vagus nerve: potential therapeutic implications of vagus nerve stimulation. J Physiol. 2016 10 15;594(20):5781–90. [PubMed: 27059884]
4. Tracey KJ. Reflexes in Immunity. Cell. 2016;164(3):343–4. [PubMed: 26824649]
5. Pavlov VA, Tracey KJ. Neural regulation of immunity: molecular mechanisms and clinical translation. Nat Neurosci. 2017 20, 156–166 [PubMed: 28092663]
6. Tracey KJ. The inflammatory reflex. Nature. 2002;
7. Borovikova LV, Ivanova S, Zhang M, Yang H, Botchkina Gl, Watkins LR, et al. Vagus nerve stimulation attenuates the systemic inflammatory response to endotoxin. 2000;405(5).
8. Olofsson PS, Rosas-Ballina M, Levine YA, Tracey KJ. Rethinking inflammation: neural circuits in the regulation of immunity. Immunol Rev. 2012 7;248(1):188–204. [PubMed: 22725962]
9. Koopman FA, Chavan SS, Miljko S, Grazio S, Sokolovic S, Schuurman PR, et al. Vagus nerve stimulation inhibits cytokine production and attenuates disease severity in rheumatoid arthritis. Proc Natl Acad Sci USA. 2016; 113(29):8284–9. [PubMed: 27382171]
10. Bonaz B, Sinniger V, Hoffmann D, Clarenc D. Chronic vagus nerve stimulation in Crohn ' s disease : a 6-month follow-up pilot study. 2016; 1–6.
11. Watkins LR, Goehler LE, Relton JK, Tartaglia N, Silbert L, Martin D, et al. Blockade of interleukin-1 induced hyperthermia by subdiaphragmatic vagotomy: evidence for vagal mediation of immune-brain communication. Neurosci Lett. 1995 1 2; 183(1–2):27–31. [PubMed: 7746479]
12. Niijima A The afferent discharges from sensors for interleukin 1 beta in the hepatoportal system in the anesthetized rat. J Auton Nerv Syst. 1996 12 14;61 (3):287–91. [PubMed: 8988487]
13. Steinberg BE, Silverman HA, Robiatti S, Gunasekaran MK, Tsaava T, Battinelli E, et al. Cytokine-specific Neurograms in the Sensory Vagus Nerve. Bioelectronic Medicine. 2016;3:7–17. [PubMed: 30003120]
14. Loeb GE, Peck RA. Cuff electrodes for chronic stimulation and recording of peripheral nerve activity. J Neurosci Methods. 1996 1;64(1):95–103. [PubMed: 8869489]
15. Hofmann UG, Folkers A, Mösch F, Malina T, Menne KML, Biella G, et al. A novel high channel-count system for acute multisite neuronal recordings. IEEE Trans Biomed Eng. 2006 8;53(8): 1672–7. [PubMed: 16916102]
16. Sohal HS, Andrew J, Richard J, Clowry GJ, Konstantin V, Anthony O, et al. The sinusoidal probe: a new approach to improve electrode longevity. Front Neuroeng . 2014;7.

17. Sohal HS, Konstantin V, Andrew J, Baker SN, Anthony O. Design and Microfabrication Considerations for Reliable Flexible Intracortical Implants. Front Mech Eng Chin. 2016;2.
18. Sohal HS, Clowry GJ, Jackson A, O'Neill A, Baker SN. Mechanical Flexibility Reduces the Foreign Body Response to Long-Term Implanted Microelectrodes in Rabbit Cortex. PLoS One. 2016 10 27; 11(10):e0165606.
19. Pavlov VA, Wang H, Czura CJ, Friedman SG, Tracey KJ. The cholinergic antiinflammatory pathway: a missing link in neuroimmunomodulation. Mol Med. 2003 5;9(5–8): 125–34. [PubMed: 14571320]
20. Olofsson PS. Single-Pulse and Unidirectional Electrical Activation of the Cervical Vagus Nerve Reduces Tumor Necrosis Factor in Endotoxemia. Bioelectronic Medicine. 2015;
21. Seymour JP, Elkasabi YM, Chen H-Y, Lahann J, Kipke DR. The insulation performance of reactive parylene films in implantable electronic devices. Biomaterials. 2009 10;30(31):6158–67.
22. Yu H, Xiong W, Zhang H, Wang W, Li Z. A cable-tie-type parylene cuff electrode for peripheral nerve interfaces. In: 2014 IEEE 27th International Conference on Micro Electro Mechanical Systems (MEMS) 2014.
23. Lee S, Yen S- C, Sheshadri S, Delgado-Martinez I, Xue N, Xiang Z, et al. Flexible Epineural Strip Electrode for Recording in Fine Nerves. IEEE Trans Biomed Eng. 2016 3;63(3):581–7. [PubMed: 26276980]
24. Badia J, Raspopovic S, Carpaneto J, Micera S, Navarro X. Spatial and Functional Selectivity of Peripheral Nerve Signal Recording With the Transversal Intrafascicular Multichannel Electrode (TIME). IEEE Trans Neural Syst Rehabil Eng. 2016 1;24(1):20–7. [PubMed: 26087496]
25. Lee S, Sheshadri S, Xiang Z, Delgado-Martinez I, Xue N, Sun T, et al. Selective stimulation and neural recording on peripheral nerves using flexible split ring electrodes. Sens Actuators B Chem. 2016 242:1165–1170
26. Seo D, Neely RM, Shen K, Singhal U, Alon E, Rabaey JM, et al. Wireless Recording in the Peripheral Nervous System with Ultrasonic Neural Dust. Neuron. 2016 8 3;91(3):529–39. [PubMed: 27497221]
27. Kagaya M, Lamb J, Robbins J, Page CP, Spina D. Characterization of the anandamide induced depolarization of guinea-pig isolated vagus nerve. Br J Pharmacol. 2002 9; 137(1):39–8. [PubMed: 12183329]
28. Scholvin J, Kinney JP, Bernstein JG, Moore-Kochlacs C, Kopell N, Fonstad CG, et al. Close-Packed Silicon Microelectrodes for Scalable Spatially Oversampled Neural Recording. IEEE Trans Biomed Eng. 2016 1;63(1): 120–30. [PubMed: 26699649]
29. Harper AA, Lawson SN. Electrical properties of rat dorsal root ganglion neurones with different peripheral nerve conduction velocities. J Physiol. 1985 2;359:47–63. [PubMed: 2987489]
30. Steffens H, Dibaj P, Schomburg ED. In vivo measurement of conduction velocities in afferent and efferent nerve fibre groups in mice. Physiol Res. 2012 1 31 ;61 (2):203–14. [PubMed: 22292724]
31. Tyler DJ, Durand DM. Chronic response of the rat sciatic nerve to the flat interface nerve electrode. Ann Biomed Eng. 2003 6;31(6):633–42. [PubMed: 12797612]
32. Graczyk EL, Schiefer MA, Saal HP, Delhaye BP, Bensmaia SJ, Tyler DJ. The neural basis of perceived intensity in natural and artificial touch. Sci Transl Med. 2016 10 26;8(362):362ra142.
33. Schiefer MA, Freeberg M, Pinault GJC, Anderson J, Hoyen H, Tyler DJ, et al. Selective activation of the human tibial and common peroneal nerves with a flat interface nerve electrode. J Neural Eng. 2013 0ct;10(5):056006. [PubMed: 23918148]
34. Schiefer MA, Tyler DJ, Triolo RJ. Probabilistic modeling of selective stimulation of the human sciatic nerve with a flat interface nerve electrode. J Comput Neurosci. 2012 8;33(1): 179–90. [PubMed: 22222951]
35. Fisher LE, Tyler DJ, Anderson JS, Triolo RJ. Chronic stability and selectivity of four-contact spiral nerve-cuff electrodes in stimulating the human femoral nerve. J Neural Eng. 2009 8;6(4):046010. [PubMed: 19602729]

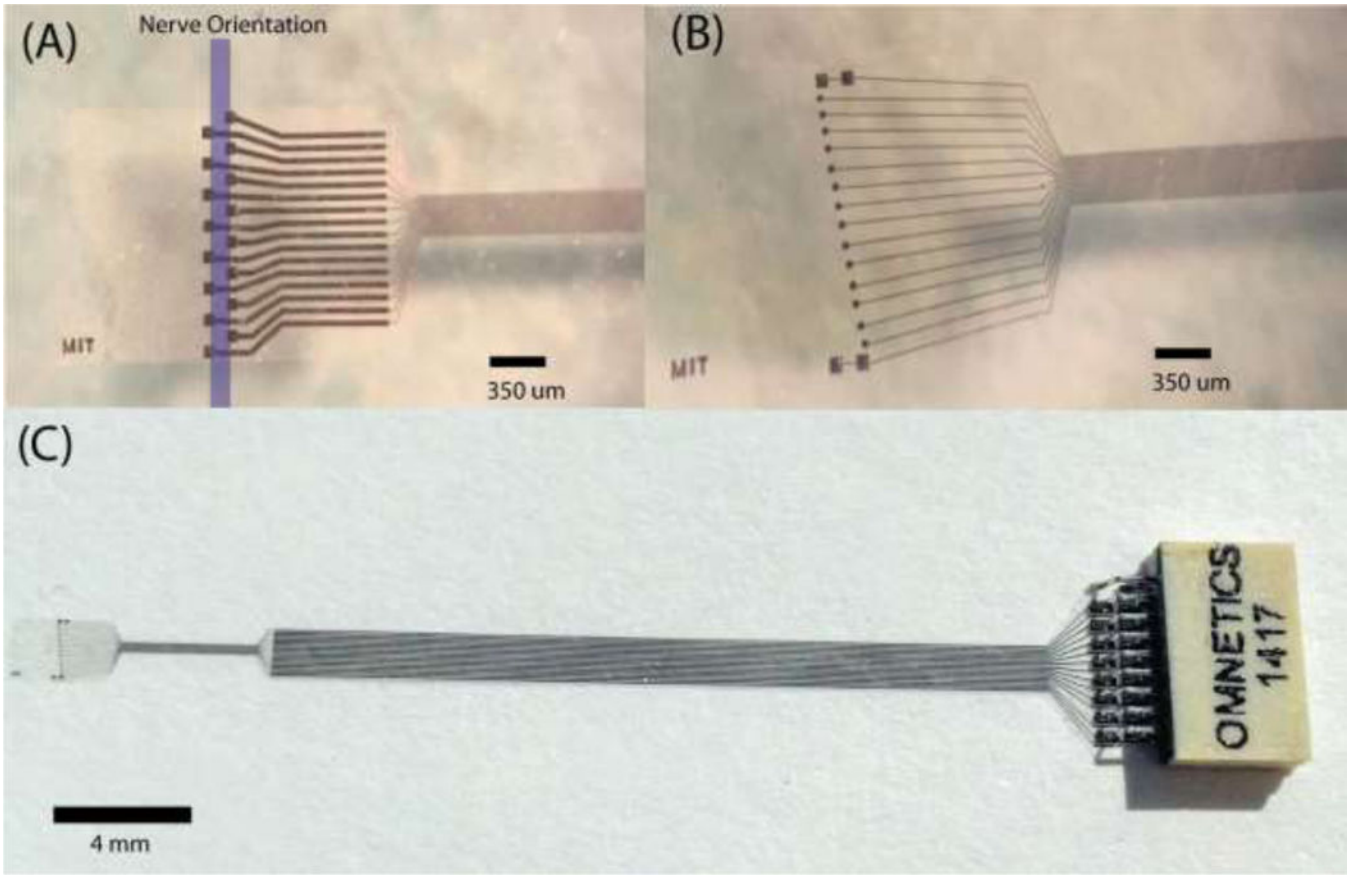

Figure 1.

Microelectrode designs for the peripheral implant in the mouse. (a) A tetrode like electrode format with the direction of the nerve, recording site area 6400 μm^2. The oversized flap wraps around the nerve and is secured in place with the use of sutures or surgically approved adhesives. (b) The diagonal format of recording sites (2500 μm^2) with two macro stimulation sites (6400 μm^2) at either end. (c) The microelectrode shown with incorporated ribbon cable and connector.

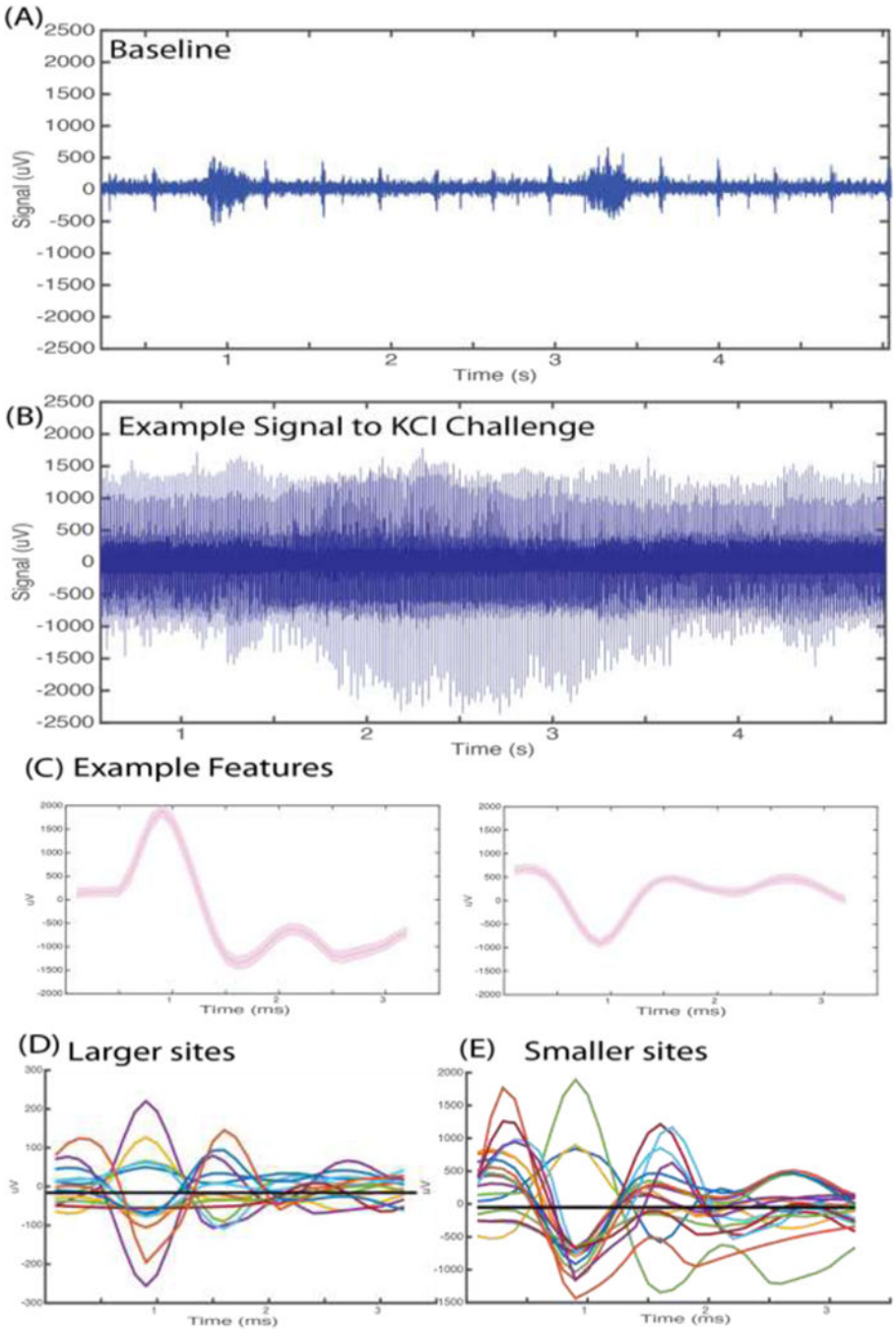

Figure 2.

Electrical vagus nerve activity in response to potassium chloride (KCI). Anesthetized mice were implanted with a microelectrode on the left cervical vagus nerve. Data was continuously acquired at 30 kHz sampling rate. (A) Example of 200 Hz high passed signal of recorded baseline activity. Burst activity synchronous with pulse and respiration was observed. (B) Example of 200 Hz high passed signal of vagus nerve activity upon cervical vagus nerve exposure to 4 mM KCI. (C) Representative features extracted from the raw signal recording upon KCI challenge. (D) Mean waveforms of CAPs extracted from activity

recorded at the 6400 μm^2 recording sites. (E) Mean waveforms of CAPs extracted from activity recorded at 2500 μm^2 recording sites.

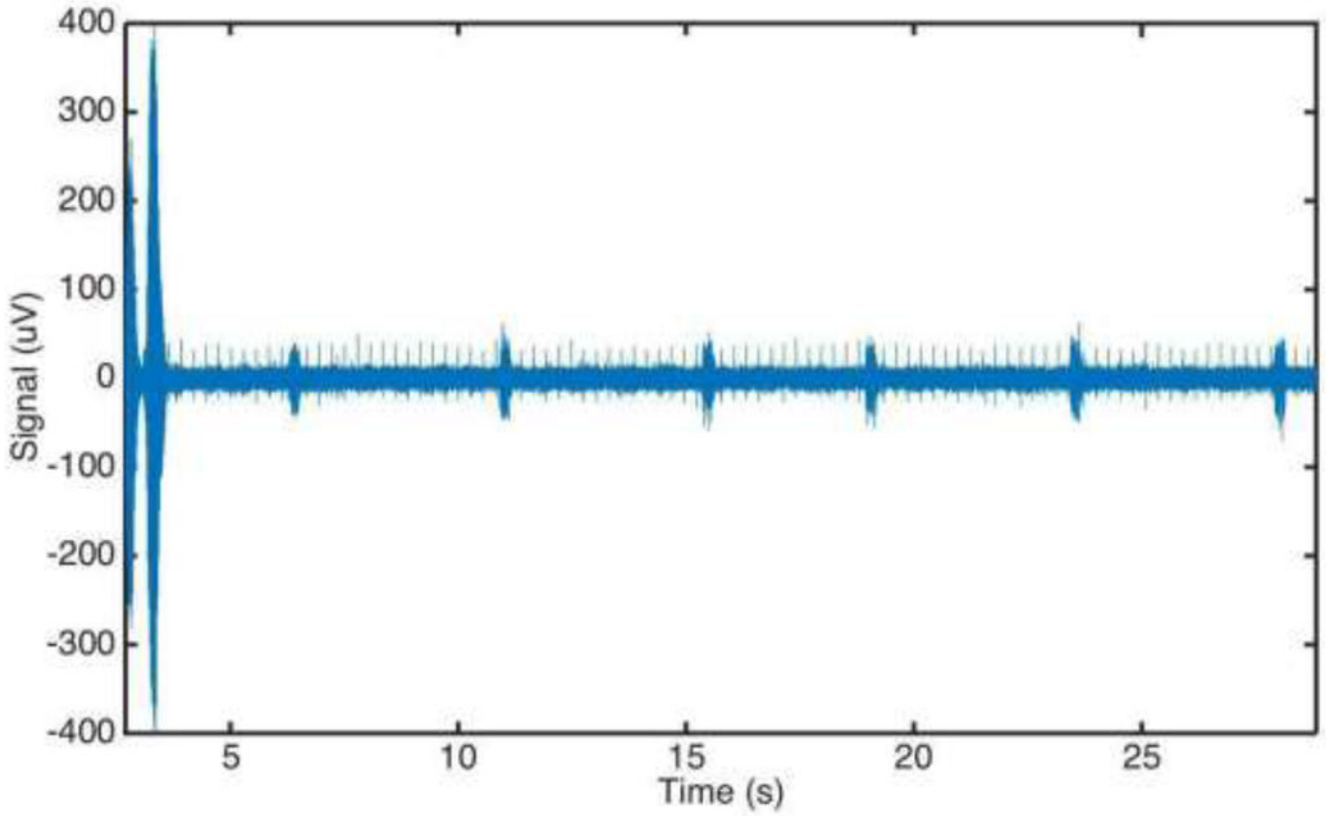

Figure 3.

Electrical cervical vagus nerve activity following intraperitoneal injection of saline. Anesthetized mice were implanted with a microelectrode on the left cervical vagus nerve. Data was continuously acquired at 30 kHz sampling rate. Injection was performed at time '0'. A movement artifact from the injection is visible in the first 5 seconds post-injection.

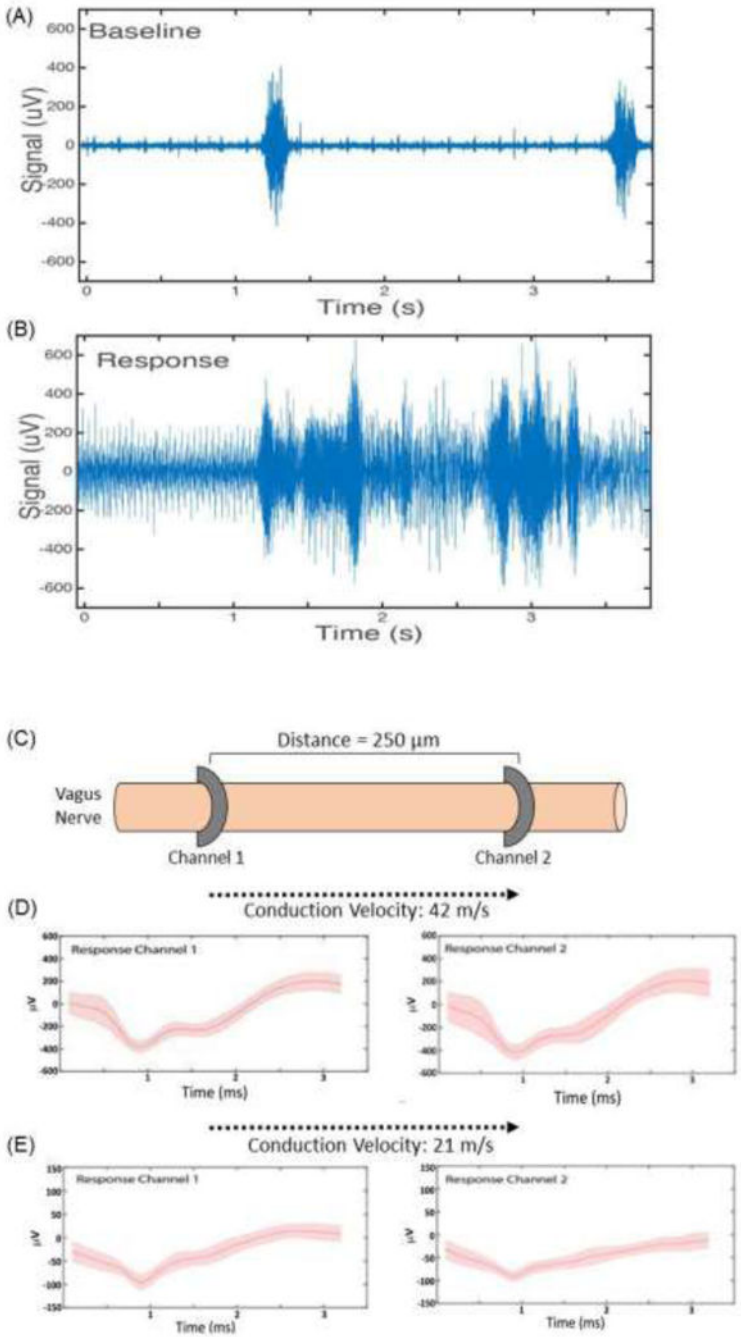

Figure 4.

Electrical vagus nerve activity in response to interleukin-1β injection. (A) Baseline electrical activity in anesthetized mice recorded from a microelectrode on the left vagus nerve. (B) Electrical activity over a 3 second time period, 5 minutes after intraperitoneal injection of IL- 1β. (C) Schematic of microelectrode placement along the cervical vagus nerve. (D, E) Features were extracted and CAPs isolated across multiple channels. Two examples are shown. The time delay in capturing these signal across the channels was used to calculate conduction velocity.

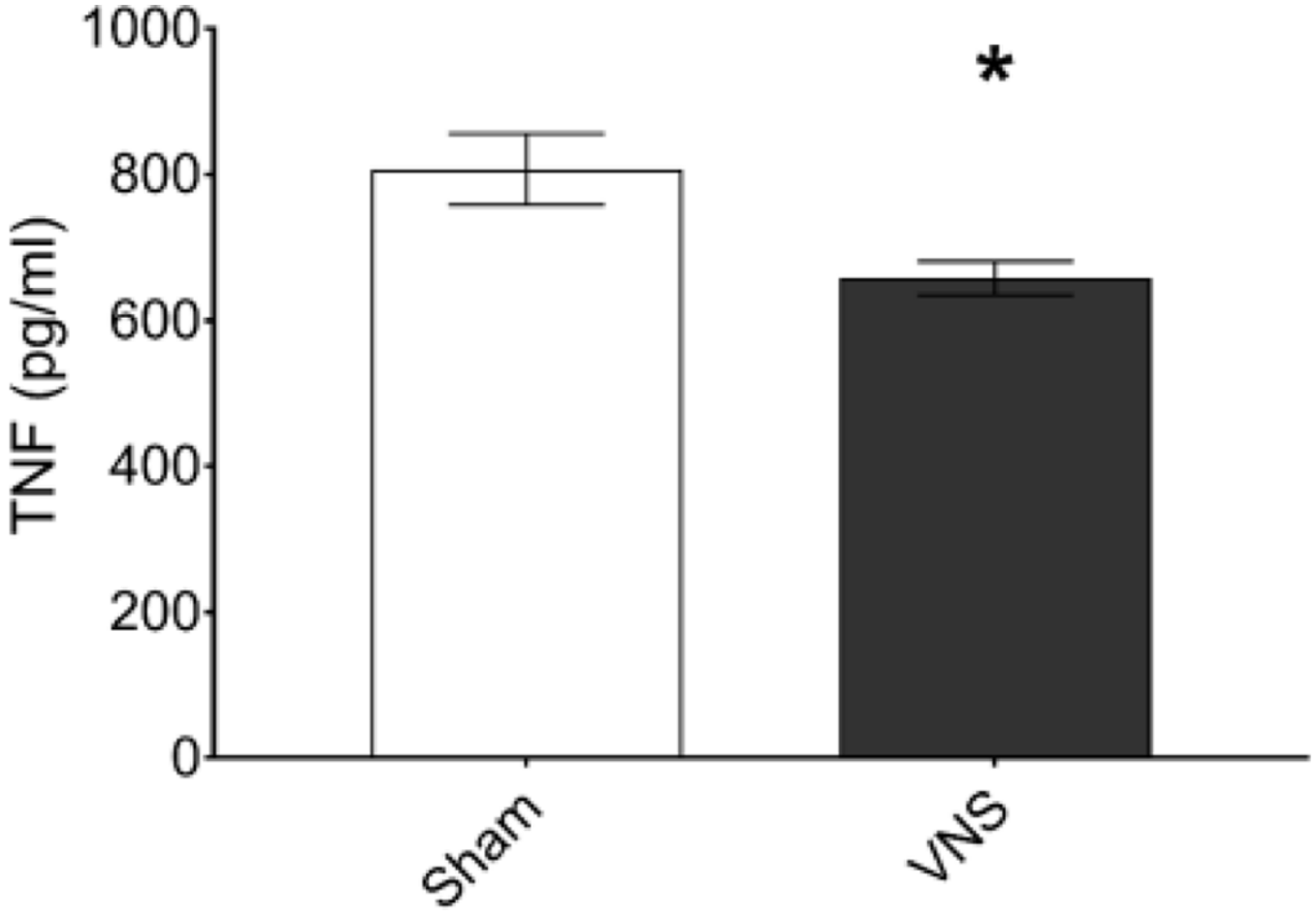

Figure 5.

Vagus nerve stimulation in a mouse model of endotoxemia. Anesthetized mice were implanted with a microelectrode on the left cervical vagus nerve and electrical stimulation performed with the following settings: 1 mA output current, 250 μs biphasic pulse width, 50 μs interphase delay at a 10 Hz pulse frequency was applied across the two 80 × 80 microelectrode contact sites for 60 seconds and endotoxin injected intraperitoneally after three hours of recovery. Serum was collected 90 minutes post-injection and TNFα was analysed by ELISA (n=30, *p<0.05, unpaired, two-tailed, Student's *t*-test).

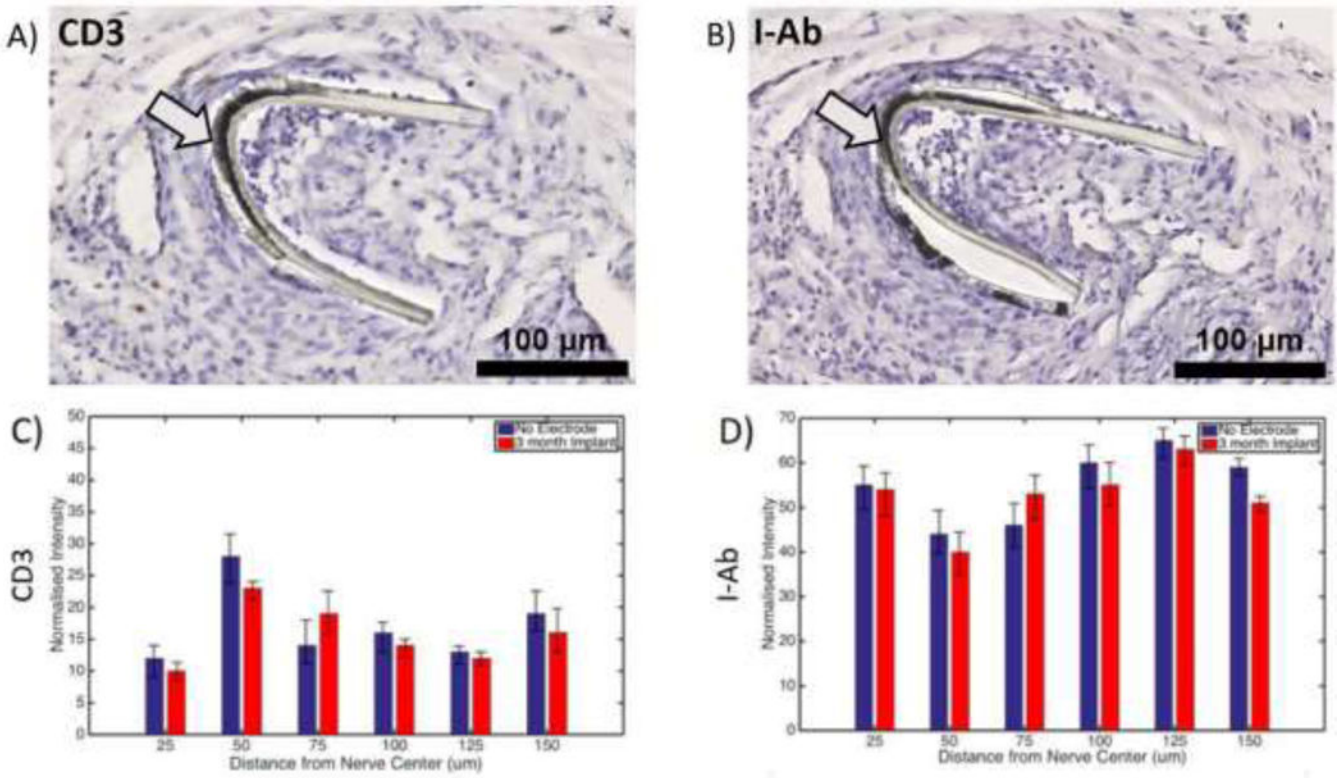

Figure 6.

Limited inflammation at the microelectrode implantation site. Mice were implanted with a microelectrode on the left cervical vagus nerve. The tissue was collected 12 weeks later and stained using anti-CD3 and anti-l-Ab antibodies. Examples of images for (A) anti-CD3 and (B) anti-l-Ab staining are shown. Arrows point to electrode. Black scale bars depict 100 µm. No significant differences were found in the radial distribution of (C) anti-CD3 or (D) anti-l-Ab staining between the 12 week implanted site and the non-implanted site across 150 um of the nerve diameter.